

ORIGINAL ARTICLE

Assessing Similarity Among Individual Tumor Size Lesion Dynamics: The CICIL Methodology

Nadia Terranova^{1*}, Pascal Girard¹, Konstantinos Ioannou¹, Ute Klinkhardt² and Alain Munafo¹

Mathematical models of tumor dynamics generally omit information on individual target lesions (iTLS), and consider the most important variable to be the sum of tumor sizes (TS). However, differences in lesion dynamics might be predictive of tumor progression. To exploit this information, we have developed a novel and flexible approach for the non-parametric analysis of iTLS, which integrates knowledge from signal processing and machine learning. We called this new methodology Classification Clustering of Individual Lesions (CICIL). We used CICIL to assess similarities among the TS dynamics of 3,223 iTLS measured in 1,056 patients with metastatic colorectal cancer treated with cetuximab combined with irinotecan, in two phase II studies. We mainly observed similar dynamics among lesions within the same tumor site classification. In contrast, lesions in anatomic locations with different features showed different dynamics in about 35% of patients. The CICIL methodology has also been implemented in a user-friendly and efficient Java-based framework.

CPT Pharmacometrics Syst. Pharmacol. (2018) 7, 228–236; doi:10.1002/psp4.12284; published online 21 February 2018.

Study Highlights

WHAT IS THE CURRENT KNOWLEDGE ON THE TOPIC?

Conventional clinical models of tumor dynamics use the total TS as a continuous variable to model the tumor time-course following anticancer therapy. Instead, considering differences among iTLS in their response to treatment provides new quantitative insights on tumor heterogeneity and disease progression.

WHAT QUESTION DID THIS STUDY ADDRESS?

A novel and flexible methodology for the non-parametric analysis of iTLS allowed the assessment of the similarity among lesion dynamics at different levels.

WHAT THIS STUDY ADDS TO OUR KNOWLEDGE

Considering that the total TS does not allow to capture tumor heterogeneity. However, lesions showing similar dynamics can be grouped to focus on and describe different tumor lesion responses while reducing the complexity of the analysis.

HOW MIGHT THIS CHANGE CLINICAL PHARMACOLOGY AND THERAPEUTICS

The CICIL methodology can be used efficiently to analyze and understand large-scale datasets prior to modeling. The results can then guide the modeler in determining whether the dynamics of iTLS, rather than the total TS, should be considered for a particular case study and for the questions to be addressed.

Over the past decade, a large number of case studies have demonstrated the value of model-informed drug discovery and development (MID3) applications in improving research and development efficiency. The clear benefits of MID3 integration with research and development programs, processes, and planning have fostered its adoption by regulatory authorities.¹

In oncology drug development, MID3 relies on a variety of models, including disease progression, pharmacokinetics, and pharmacodynamics, for improving quantitative, informed decision-making, and regulatory evaluations.^{2,3} Added benefits have been gained from mathematical models of tumor size (TS) dynamics^{4–6} and tumor growth inhibition,^{7–9} which can characterize anticancer drug effects over time and provide improved predictors of long-term clinical outcomes.^{10,11}

Clinical models of tumor dynamics use the total TS as a continuous variable to model the tumor time-course. The total TS is estimated as the sum of diameters (in the case

of unidimensional measures) or the sum of products of diameters (in the case of bidimensional measures) for all target lesions in a patient.¹² The total TS approach overcomes the limitations and loss of information that result from categorizing the response to treatment according to the World Health Organization (WHO) criteria^{13,14} or to the subsequently developed Response Evaluation Criteria In Solid Tumors (RECIST)¹⁵ criteria for solid tumors.¹⁶ However, the total TS represents only an average measure that reflects mainly the gross behavior of the largest lesion(s) in a patient. Indeed, the total TS is a highly approximated measure that does not capture differences in tumor dynamics of individual target lesions (iTLS), their number, and their locations. This omitted information could be relevant to tumor differentiation or resistance-related mechanisms.¹⁷ In particular, differences among tumor lesions in their response to treatment might provide new quantitative insights on tumor heterogeneity (e.g., genetic/epigenetic alterations,

¹Merck Institute for Pharmacometrics, Merck Serono S.A., Switzerland, a Subsidiary of Merck KGaA, Darmstadt, Germany; ²Merck KGaA, Darmstadt, Germany.

*Correspondence: N Terranova (nadia.terranova@merckgroup.com)

Received 11 October 2017; accepted 17 January 2018; published online on 21 February 2018. doi:10.1002/psp4.12284

nature of microenvironmental composition, and cell activation states) within a given tissue or among different tissues,¹⁸ and/or predict differences in disease progression.^{19,20} Thus, a tool for comparing lesion dynamics prior to modeling is important to assess whether the total TS can reasonably capture the tumor lesion response. This should be based on a flexible method that allows a rapid analysis of longitudinal TS data from iTLs and provides an efficient overview of results from large-scale studies.

For this purpose, we have integrated existing techniques from other fields into a new methodology called Classification Clustering of Individual Lesions (CICIL). In particular, CICIL relies on the classification of iTLs based on functional and anatomical criteria, defined by current medical knowledge, and it is based on a workflow accommodating the assessment of the similarity among lesion dynamics, through cross-correlation measures of classified lesions.²¹ Interpretation of the results is then facilitated with the k-means clustering.²² Taken together, this methodology provides a better understanding and quantification of the information available in the considered dataset. Indeed, by combining information on iTLs with TS data, results allow to assess whether a total TS evaluation might reasonably predict tumor lesion behavior, or potential differences in responses, within or across tumor site classes, should be taken into account.

MATERIALS AND METHODS

Trials and data

We retrieved TS data of iTLs measured in patients with irinotecan-resistant epidermal growth factor receptor expressing metastatic colorectal cancer (mCRC). Patients had been enrolled in the MABEL (Monoclonal Antibody Erbitux IN A European pre-License study; electronic medical record 62202-501)²³ or EVEREST (Evaluation of Various Erbitux REgimens by means of Skin and Tumor biopsies; electronic medical record 62202-502)²⁴ studies, which tested cetuximab in combination with irinotecan. In the uncontrolled phase II MABEL study (hereafter defined as study 1), a total of 1,147 patients were treated with cetuximab (starting dose of 400 mg/m², then a weekly dose of 250 mg/m²) plus irinotecan, in the following dosage regimens: 125 mg/m² weekly for 4 consecutive weeks, followed by 2 weeks rest; 180 mg/m² every 2 weeks; or 350 mg/m² every 3 weeks. Tumor lesions were evaluated at baseline, every 12 weeks during study treatment, and at the end of study visit. In the phase I/II EVEREST study (hereafter defined as study 2), cetuximab was administered in combination with irinotecan (180 mg/m² every 2 weeks) to 157 patients. Patients had been randomized to the standard cetuximab regimen or to a dose escalation regimen (from 300 mg/m² to 500 mg/m², increased by 50 mg/m² every 2 weeks). Tumor lesions were assessed at baseline, every 6 weeks thereafter, at the end of treatment visit, and at the end of study visit (i.e., 6 weeks after the last treatment).

In both studies, imaging for tumor assessment was performed, either by computed tomography scan or magnetic resonance imaging scan. Tumor responses were classified according to modified WHO criteria. At baseline, target (or

index) lesions were defined as measurable lesions representative of all involved organs, with a maximum of 5 lesions per organ, and 10 lesions in total. Target lesions were bidimensionally measured, and size was estimated as the product of the longest diameter and its perpendicular diameter. In addition to the recorded TS measures over time, information about the tumor site and tumor type (i.e., primary, node, or metastasis) was collected for each target lesion. These data were recorded in the study case report form, as free text and a pre-defined code, respectively. The sum of the diameter products of iTLs selected as target lesions and the recorded information on non-target lesions and new lesions were used to derive response and progression outcomes throughout the studies.

THE CICIL METHODOLOGY

The CICIL methodology has a novel, flexible workflow that promotes efficient assessments of similarities of lesion dynamics on large-scale datasets in a non-parametric manner. It comprises three main sequential steps.

Rule-based classification

Intra-tumor and inter-tumor heterogeneity is characterized by considerable variations in genetic makeup, aggressiveness, and drug sensitivity.²⁵ Hence, heterogeneity actively influences the therapeutic tumor response and shapes drug resistance. In addition, the specific tumor microenvironment contributes to the uniqueness of each tumor lesion.²⁶ Therefore, we used the tissue description and the tumor type reported for each iTL to develop a new classification of tumor lesions, based on the anatomical location and different reported features. In particular, our classifications focused on the tumor types and tumor metastasis sites typically observed in patients with mCRC. Lesions described as primary were classified differently from lesions described as a node (class #100 and class #3, respectively, in **Table 1**). The classification of a metastatic lesion was based on the known pattern of target organ metastasis, with specific classes assigned to different metastatic sites typically observed in mCRC, and characterized by different properties (e.g., the lung is defined as class #2). Instead, less frequently reported sites were classified according to the organ system, as reported in the International Classification of Diseases,²⁷ and by also considering the vascular anatomy and tumor microenvironment. Tumor sites with similar properties were then nested, and successively lumped into main, well-represented classes. For instance, classes for lesions in the small intestine/duodenum, large intestine/rectum, retroperitoneum/peritoneum, or in other digestive organs were merged into a more general class of "Other digestive organs and peritoneum" (**Figure 1**). As reported in **Table 1**, this process led to the definition of 10 main classes, each primarily representative of one specific class of tumor identified in both studies.

Free-text descriptions of tumor sites recorded by physicians in the study case report forms were based on non-standardized entries, which reported various specific physiological/anatomical terms. In order to use this information in lesion

Table 1 Classification of iTLs from study 1 and study 2

| Class # | Class description | Type | Study 1 No. of lesions ^a | Study 2 No. of lesions ^a |
|------------------------------------|---|------------|--|--|
| 1 | Liver | Metastasis | 674 (1,628) | 129 (337) |
| 2 | Lung | Metastasis | 298 (634) | 57 (107) |
| 3 | Lymph node | Node | 119 (188) | U |
| 4 | Bone/bone marrow | Metastasis | U | U |
| 5 | Brain/spinal cord/other parts of nervous system | Metastasis | - | - |
| 6 | Other respiratory and intrathoracic organs/structures | Metastasis | 31 (40) | U |
| 7 | Other digestive organs and peritoneum | Metastasis | 77 (105) | U |
| 8 | Other specified organs | Metastasis | U | U |
| 100 | Primary (and locally advanced tumors) | Primary | U | U |
| 999 | Other/non-specified | Metastasis | 96 (113) | 36 (71) |
| TOTAL NUMBER OF INDIVIDUAL LESIONS | | | 1,295 (2,708) | 222 (515) |

iTLs, individual target lesions; cTLs, class-related target lesions.

^aThe number of cTLs derived for the inter-class analysis (one per patient) is reported; the number of all iTLs (>1 per patient) is shown in parentheses.
U = Under-represented classes (i.e., including lesions from <20 patients) reassigned to other classes during the second classification step.

classifications, we defined a list of keywords representative of the involved sites for each class. We then developed a rule-based classifier that could automatically classify iTLs based on the recorded code type and recognition of predefined keywords in the description (**Figure 1**). We implemented this automatic classifier in SAS software 9.3 (Copyright 2002–2010 SAS Institute).

Cross-correlation analysis

A comparison of lesion TS dynamics involves a large amount of data: each single patient might have multiple

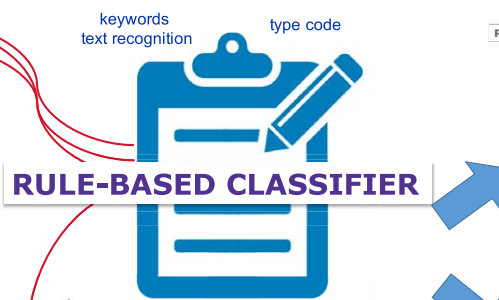
iTLs, and each lesion is measured at multiple assessment visits. Hence, this analysis requires a methodological approach for handling large-scale datasets and providing concise and construable output information that could also be used at the study/population level.

Inspired by the analogy between tumor time profiles and signals, we conducted a cross-correlation analysis to assess similarities among tumor lesion dynamics in a non-parametric manner. The cross-correlation analysis is a standard, well-recognized methodology in signal processing and it is used to estimate the degree of correlation between

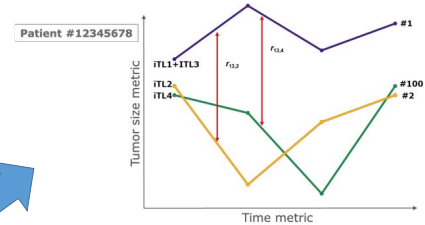
NEW CLASSIFICATION

| Class # | Class description |
|---------|---|
| 1 | Liver |
| 2 | Lung |
| 3 | Lymph Node |
| 4 | Bone/bone marrow |
| 5 | Brain/Spinal cord/other parts of nervous system |
| 6 | Other respiratory and intrathoracic organs/structures |
| 6.1 | Mediastinum |
| 6.2 | Pleura, other respiratory organs |
| 7 | Other digestive organs and peritoneum |
| 7.1 | Small intestine/duodenum |
| 7.2 | Large intestine/rectum |
| 7.3 | Other digestive organs |
| 7.4 | Retropertoneum/peritoneum |
| 8 | Other specified sites |
| 8.1 | Kidney/renal pelvis |
| 8.2 | Other urinary organs |
| 8.3 | Ovary |
| 8.4 | Adrenal gland |
| 8.5 | Breast |
| 8.6 | Genital organs |
| 8.7 | Sin/muscle |
| 999 | Other/non-specified |
| 100 | Primary |

Case Report Form



INTER-CLASS



INTRA-CLASS

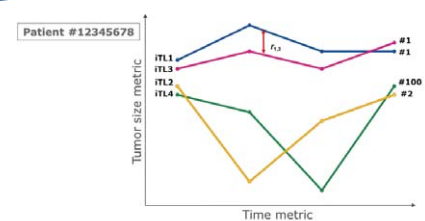


Figure 1 The developed rule-based classifier allows to automatically classify individual target lesions (iTLs), based on the recorded tumor type and free-text description reported in the case report form. In the illustrated example, patient's lesions iTL1 and iTL3 were identified as belonging to the liver and assigned to class #1, lesion iTL2 was assigned to class #2 representative of the lungs, and lesion iTL4 to the class #100 of primary tumors. The lesion classification then allows to perform: (i) the inter-class analysis to compare the tumor size (TS) dynamics among lesions of different classes, and, in particular, between the largest lesion at baseline (given by the sum of iTL1 and iTL3) and those assigned to the other classes (class #1 vs. #2, class #1 vs. #100); (ii) the intra-class analysis to compare TS dynamics of lesions iTL1 and iTL3 assigned to the same class.

two series at shifted sampling times.²¹ We assume lesion dynamics to be wide-sense stationary time series with constant means. Although, in reality, tumor dynamics means could not be constant, we consider this simplifying assumption to be reasonable in practice as tumor doubling time is usually extremely slow. Hence, the cross-correlation between series, or tumor dynamics that are aligned or shifted in time, can be measured by computing the cross-correlation coefficient (CC).

The CC between a pair of time series is defined as the cross-covariance normalized by the standard deviations (SDs) of the series. More formally, given two time series X_t and Y_t , the CC at sample time shift d (also known as lag) can be computed as follows:

$$r_{xy}(d) = \frac{1}{\sigma_x \sigma_y} E[(X_t - \mu_x)(Y_{t-d} - \mu_y)] = \frac{\gamma_{xy}(d)}{\sigma_x \sigma_y} \quad (1)$$

where $\gamma_{xy}(d)$ is the cross-covariance, μ_x and μ_y are the means of the corresponding series, σ_x and σ_y are the SDs, and $E[\]$ indicates the expected value.

The CC can be estimated by computing the sample CC $\hat{r}_{xy}(d)$, at time shift d , on sample series $x = \{x_1, \dots, x_n\}$ and $y = \{y_1, \dots, y_n\}$ as the average product of the samples observed from X_t and the samples observed from Y_t at its time shift:

$$\hat{r}_{xy}(d) = \frac{1}{n} \sum_{i=1}^n \frac{(x_i - \bar{x})(y_{i-d} - \bar{y})}{s_x s_y} \quad (2)$$

where n is the number of pairs of samples, \bar{x} and \bar{y} are the sample series means, and s_x and s_y are the sample series SDs.

For two sample series, x and y , $\hat{r}_{xy}(d)$ provides an approximate measure of similarity between the series, with y delayed by d samples. The CC values range from -1 to 1 ; these boundaries indicate the presence of opposite profiles (i.e., a value of -1 indicates that one profile increases and the other decreases with time) and completely parallel profiles (i.e., a value of 1 indicates profiles that similarly increase or decrease with time). When the CC is computed for all time shifts ($d = 0, \pm 1, \dots, \pm n-1$), a cross correlation set of $2n-1$ coefficients is obtained. Lagged CCs allow one to identify at which sample shift the maximum correlation between series is observed, and to verify whether the profile of one series can be considered delayed with respect to the other series.

The *ccf* function provided in the Stats package of R software version 3.1 (Copyright 2014; The R Foundation for Statistical Computing) was used to derive CCs between pairs of target lesion dynamics for each subject in the two studies considered. Missing assessments of tumor lesions were investigated beforehand to ensure that subject lesions were measured at the same sampling (i.e., scheduled) time, and, thus, avoid erroneous comparisons. No missing values were identified before the last tumor assessment. Therefore, no imputation rule had to be implemented and no measures had to be disregarded. In this respect, it is worth noting that, for the calculations of CC sets in a given

patient, a missing tumor measure for one iTL, which would have resulted in the omission of the total TS at that specific assessment, would not lead to the complete omission of the other corresponding iTL measures. Indeed, a tumor observation at a specific assessment time would not be considered in comparisons involving a lesion missing that assessment, but it would be used in the calculation of CCs for the other tumor lesions.

K-means clustering analysis

We used k-means clustering²² to support and facilitate the interpretation of similarity measures for each pair of lesions at different sampling times. In particular, this partitioning method was used to group the CCs to then, assess possible differences in cluster centers and distributions in a straightforward way.

The iterative k-means algorithm is a common, simple centroid-based clustering method. It finds the best division of entities, here, the CCs, into k clusters by minimizing the within-cluster sum of squares as follows:

$$\arg \min_S \sum_{i=1}^k \sum_{e \in S_i} \|e - \mu_i\|^2 \quad (3)$$

Here, μ_i is the centroid (i.e., the representative CC) of the i -th cluster, and S_i is the set of entities e , that belong to cluster i .

We performed k-means clustering with the *kmeans* R function. After exploring the within-cluster sum of squares with different numbers of clusters, we selected the best number to be three clusters.

RESULTS

iTL classification

We applied the rule-based classifier that we had developed to analyze the descriptions of 3,223 iTLs from 1,056 subjects, having at least two available TS assessments. Specifically, the classification involved 2,708 iTLs from 902 subjects, from study 1, and 515 iTLs from 154 subjects from study 2.

We considered only well-represented classes by performing a two-step classification strategy. The first step assessed the lesion and subject distributions; the second step re-classified iTLs after excluding classes that contained lesions from <20 patients. For study 1, the second classification step consisted of redistributing lesions in primary tumors into classes that represented the corresponding CRC location of metastasis, and in combining the under-represented class, “bone/bone marrow,” with the two general classes, “Other/specified” and “Other/non-specified,” into a unique general class called “Other/non-specified.” For study 2, all iTLs in under-represented classes were re-assigned to the general class “Other/non-specified.”

The second classification step resulted in six and three classes representative of tumor lesions, in study 1 and study 2, respectively. Obtained subject and iTL distributions across classes are reported in **Table 1** for both studies. Note that classes that represented typical sites of mCRC (i.e., liver and lungs) included the highest numbers of iTLs;

Table 2 Inter-class k-means clustering of the CCs measured at the zero time shift and of the maximum CCs for study 1 and study 2

| | Study 1 | | | | Study 2 | | | |
|-----------|---------------------------------|---------|-------------|---------|---------------------------------|---------|-------------|---------|
| | CCs measured at zero time shift | | Maximum CCs | | CCs measured at zero time shift | | Maximum CCs | |
| | Center | Size, % | Center | Size, % | Center | Size, % | Center | Size, % |
| Cluster 1 | -0.899 | 23 | -1 | 15 | -0.802 | 19 | -1 | 9 |
| Cluster 2 | 0.071 | 11 | 0.442 | 20 | 0.327 | 16 | 0.479 | 23 |
| Cluster 3 | 0.944 | 67 | 0.959 | 65 | 0.929 | 65 | 0.93 | 68 |

CCs, cross-correlation coefficients.

thus, supporting the appropriateness of the defined classification criteria.

The degree of similarity among lesion dynamics was then assessed with two different approaches. We analyzed lesions of different classes (inter-class analysis), and lesions in the same classes (intra-class analysis) within a subject (see the example in **Figure 1**). In the inter-class analysis, the sum of TS of iTLs was first derived for all classes within a subject. The TS dynamics of resulting class-related lesions (hereafter defined as cTLs) were then compared. Hence, the distribution of cTLs involved in this analysis corresponded to the respective subject distribution across classes. Furthermore, the total number of cTLs included in the inter-class analysis for both studies only slightly decreased after the second classification. Thus, the second classification did not largely determine the sum of TS of iTLs initially classified as belonging to different sites.

Assessment of similarity among classified iTL dynamics

To assess the similarity among lesion dynamics within patients, subjects with more than one classified iTL were considered in the inter-class and intra-class analyses. For each patient, the CCs between the largest lesion at baseline and every other lesion were evaluated, and k-means clustering was subsequently performed.

The inter-class analysis

The inter-class analysis involved subjects with lesions of multiple classes. The CCs were measured at different time shifts for comparisons of 614 classified cTLs from 272 subjects in study 1, and 134 classified cTLs from 65 subjects in study 2. We then performed k-means clustering on CCs measured at the zero time shift and on the CCs with the maximum values. With the available assessments, up to ± 6 and ± 10 sample shifts were analyzed for study 1 and study 2, respectively.

For both studies, results at the zero time shift highlighted different dynamics for circa, 35% pairs of lesions (CCs in clusters 1 and 2) from about 30–35% of subjects included in the inter-class analysis. Specifically, as shown in **Table 2** and **Figure 2**, a small positive correlation was observed at the zero time shift for about 11–16% of comparisons assigned to cluster 2. An additional 20% of the CCs assigned to cluster 1, with a center at or close to -1 , indicated the presence of very different, if not opposite, profiles. Quite high values were obtained for the remaining CCs assigned to cluster 3, with a center around 0.9. Higher CCs, and then similarity in tumor time-course without accounting for any

time shift, could not be further attributed to specific comparisons of tumor sites. Indeed, as shown in **Figure 3**, the percentages of CCs assigned to cluster 3 were quite similar across the pairs of considered classes, and, in particular, within the numerous classes whose percentages were similar to the overall size of cluster 3. Considering the maximum CC values measured at different shifts showed that almost 90% of comparisons were assigned to cluster 2 and cluster 3, with centers near 0.5 and above 0.9, respectively (**Figure 2** and **Table 2**).

Figure 4 shows the distribution of time shifts within clusters. Specifically, the maximum CCs in cluster 2 were obtained for relatively small shifts, and in cluster 3 maximum CCs were observed mainly at the zero time shift. The additional number of high-value CCs suggested that a similar tumor profile shifted in time is observed for these cTLs. The CC values assigned to cluster 1 (15% in study 1 and 9% in study 2), which indicated opposite TS profiles, were all measured at the zero time shift. Indeed, for these coefficients, comparisons mainly involved cTLs with only two TS assessments, thus preventing the evaluation of lesion similarity at any time shift and then a potential maximization of the correlation.

The intra-class analysis

The proposed methodological workflow was then adopted for the intra-class analysis to compare dynamics of iTLs that were similarly classified. In particular, for each considered class, we derived CCs among the classified iTLs within a given subject; then, we performed a cluster analysis with the k-means algorithm. Similar iTL dynamics were mainly indicated. Specifically, high CC values (assigned to cluster 3) were obtained for about 60–80% of CCs at the zero time shift for most of the considered classes. The percentages of CCs at the zero time shift assigned to cluster 3 are shown in **Table 3** for each considered class. As for the inter-class analysis, maximum values obtained at different shifts determined a size reduction of cluster 1 with a center at or close to -1 (**Table 3**), thus highlighting that additional iTLs would have a similar TS profile when accounting for shifted sampling times.

DISCUSSION

One of the first advantages of using iTLs is that no tumor data are omitted. Indeed, as opposite to the total TS, a missing tumor measure for one iTL would not result in the omission of all other corresponding iTLs measures. In

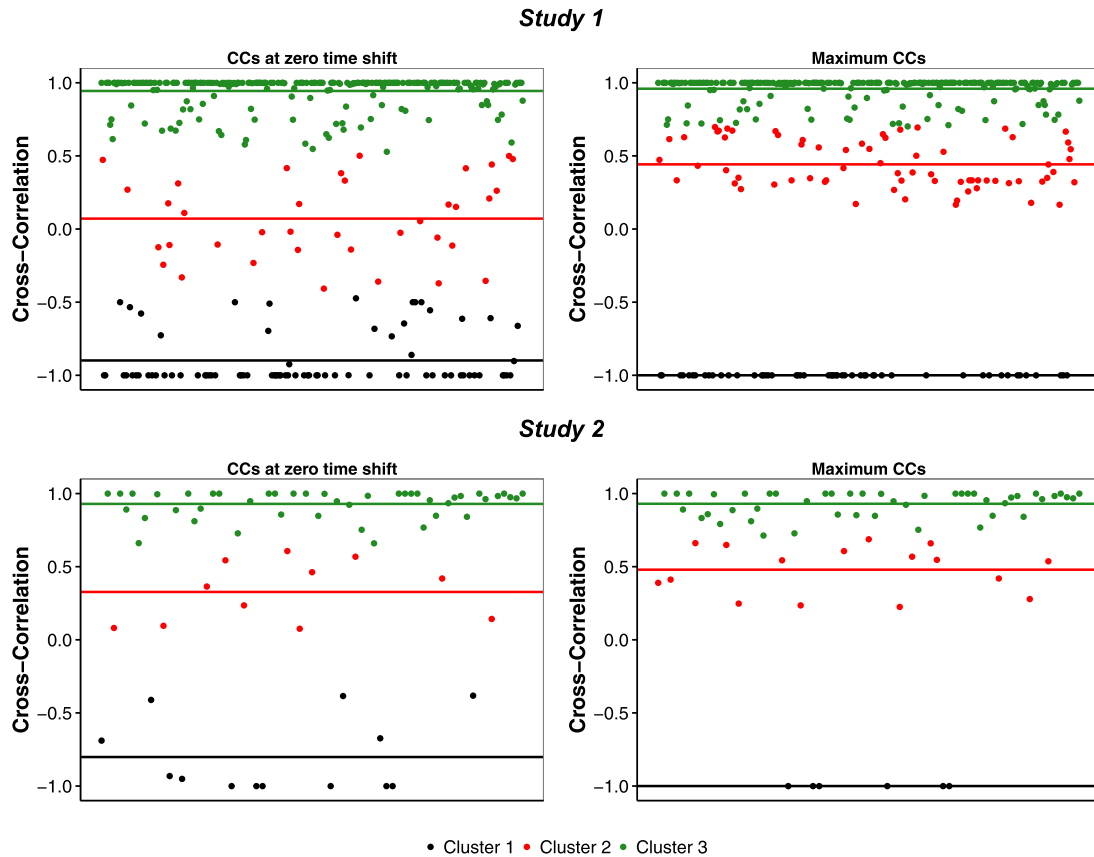


Figure 2 Inter-class analysis. The K-means clustering results are shown for study 1 (top) and study 2 (bottom). The K-means clustering was performed on cross-correlation coefficients (CCs) measured at the zero time shift (left panels) and on the maximum CC values measured at different shifts (right panels). The CCs (jittered on x-axis) assigned to cluster 1 (black dots), to cluster 2 (red dots), and to cluster 3 (green dots) are shown for each clustering analysis.

addition, combining the information on iTLs with information on lesion dynamics can provide a new quantitative understanding of the influence of tumor heterogeneity on the therapeutic response that is of particular relevance for metastatic cancers. To this end, the CICIL methodology proposes a novel and suitable workflow for the non-parametric analysis of iTLs. By being sufficiently flexible to be used for many cases, this approach allows assessments of similarity among lesion dynamics at different levels by taking advantage of tumor data collected in clinical studies. Indeed, by classifying iTLs based on the available tumor information, the CICIL methodology allows one to identify whether relevant differences in tumor responses can be attributed to heterogeneity between specific pairs of classes in the case of inter-class analyses, or to heterogeneity within a single class in cases of intra-class analyses. Specifically, for each of these analyses, results obtained at the zero time shift allows to rapidly identify differences in tumor lesion dynamics. Then, depending on the proportion of patients and lesions showing such differences, the sum of lesions TS may be considered as a reasonable approximation to describe lesions dynamics within a patient, or the modeling of iTLs may be preferred. The latter would be further informed by the investigation of lagged CCs, which may

indicate that (i) the time-course of one lesion can be considered delayed with respect to the other (i.e., if high CC values indicating similarity are obtained when accounting for a certain time shift), or (ii) more mechanistic assumptions (e.g., to describe poor drug's activity in certain tumor tissues) should be made.

The CICIL results for the two considered phase II studies indicated similar dynamics among iTLs within the same tumor site classification, and different dynamics among cTLs, which could be, in part, attributed to a tumor profile shifted in time in about 35% of patients. Thus, subsequent modeling of TS should be performed on cTLs dynamics, rather than total TS, and assumptions resulting in delayed tumor dynamics in certain tissues within a patient (e.g., different tumor growth rate or drug killing rate) should be tested to describe most of the observed differences. This would allow to better characterize the subject's response to anticancer therapy and drug's action on specific tumor tissues.

Indeed, differences in lesion dynamics might be predictive of tumor progression. Considering the total TS does not allow to capture tumor heterogeneity, then looking for differences across lesions dynamics is a crucial aspect to contemplate when developing new, convincing models of

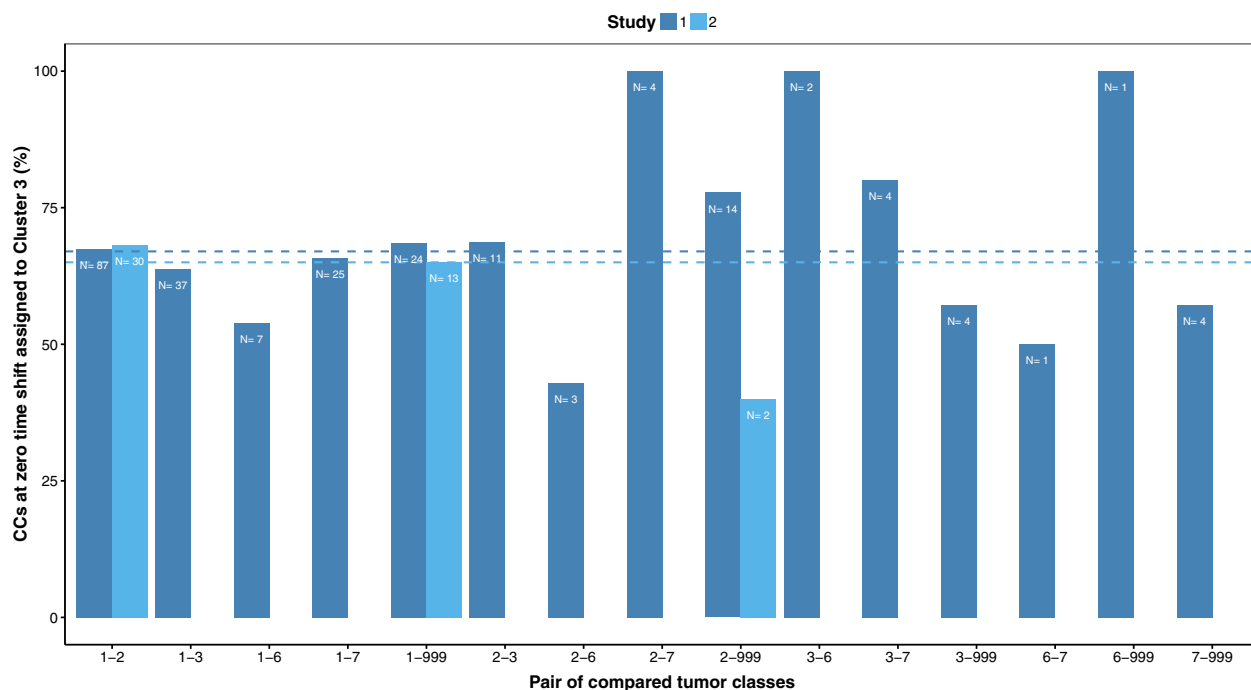


Figure 3 The percentage of cross-correlation coefficients (CCs) at the zero time shift within cluster 3 is reported for each pair of classes compared in the inter-class analysis for study 1 (classes 1, 2, 3, 6, 7, and 999) and study 2 (classes 1, 2, and 999); see **Table 1** for descriptions of classes. As a reference, overall size of cluster 3 is also shown with dashed lines for each study (67% for study 1 and 65% in study 2, see **Table 2**).

tumor dynamics and, in turn, new treatment paradigms.¹⁷ Even though the adoption of more mechanistic models might be discouraged by their complex formulation or limited availability of experimental data, we have shown that the CICIL methodology can be used efficiently to analyze and understand large-scale datasets prior to modeling, and then guide the modeler in determining the most appropriate

approach for a particular case study and for the questions to be addressed.

The proposed CICIL methodology can be easily applied to either the bidimensional product (WHO criteria), the longest diameter (RECIST criteria), or any future emergent volumetric measurement provided by progresses in tumor imaging and/or tumor size collection. Further investigations

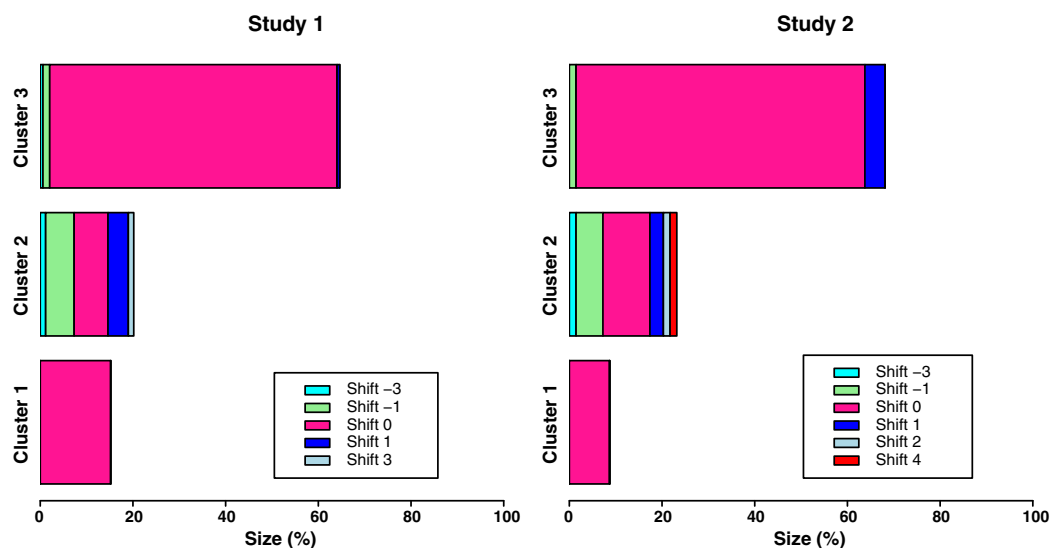


Figure 4 Distribution of time shifts at which maximum measured cross-correlation coefficients were assessed in the inter-class analysis. The percentage size of the three k-means clusters are shown for study 1 (left panel) and study 2 (right panel).

Table 3 Intra-class distributions of iTLs and the involved subjects

| Data source | Lesion classification | No. of iTLs | No. of subjects | Cluster 3 size at zero time shift, % | Size reduction for cluster 1 with maximum CCs, % |
|-------------|---|-------------|-----------------|--------------------------------------|--|
| Study 1 | Liver | 1,266 | 420 | 82 | -2 |
| | Lung | 396 | 134 | 74 | -8 |
| | Node | 86 | 33 | 58 | -9 |
| | Other respiratory and intrathoracic organs/structures | 13 | 6 | 86 ^a | NA |
| | Other digestive organs and peritoneum | 40 | 15 | 60 | -24 |
| | Other/nonspecified | 29 | 14 | 73 | -7 |
| Study 2 | Liver | 302 | 100 | 75 | -9 |
| | Lung | 78 | 31 | 53 | -24 |
| | Other/nonspecified | 47 | 16 | 39 | -13 |

The data show the percentages of CCs that indicated similar dynamics at a zero time shift (cluster 3 size), and the size reduction of cluster 1 when considering the maximum CCs.

CCs, cross-correlation coefficients; iTLs, individual target lesions; NA, not applicable.

^aPercentage of CC values in cluster 2 and cluster 3 both included high values and both had a center equal to or greater than 0.9.

should include the integration of enriched iTL data (e.g., information on biomarker and genetic mutations) from future trials, as well as data on new lesion appearance to assess relationships within and across tissues that may be predictive of disease progression.

A Java-based cross-platform implementation of the CICIL methodology has also been developed to enable a user-friendly and efficient execution, to assist the interpretation and visualization of each individual step in the workflow and to facilitate the knowledge and information sharing among different projects and users.

The CICIL tool boasts a very intuitive graphical user interface designed to accommodate an easy creation of new projects, a flawless dataset importation (csv format), and quick data manipulation. Moreover, through the graphical user interface the user can execute the CICIL workflow and customize the settings of the different components (e.g., defining the iTLs classification by using standard terms extracted from the dataset and/or user-defined keywords, performing the inter-class or intra-class analysis by optionally considering between-lesion time shifts in tumor growth dynamics). Eventually, the user can visualize and assess the CICIL methodology output and data through a series of clear plots and statistical summaries. A selective export feature enables to automatically generate customizable reports.

The CICIL tool's executable (JAR file) is available as **Supplementary Material** along with a use case based on a mock dataset. System requirements and application features are described in the respective user guide embedded in the tool and also available as **Supplementary Material**.

Acknowledgments. This work does not necessarily represent the view of all DDMoRe partners. The authors thank Paolo Magni for reviewing the manuscript prior to submission. The research leading to these results received support from the Innovative Medicines Initiative Joint Undertaking, under grant agreement number 115156; those resources were composed of financial contributions from the European Union's Seventh Framework Programme (FP7/2007–2013) and EFPIA companies, in a kind contribution. The DDMoRe project is also supported by financial

contributions from Academic and SME partners. This work does not necessarily represent the view of all DDMoRe partners.

Conflict of Interest. N.T., P.G., and A.M. are employees of Merck Serono, Switzerland, a subsidiary of Merck KGaA, Darmstadt, Germany. K.I. from the School of Computer and Communication Science of EPFL was performing an internship at the Merck Institute of Pharmacometrics, Lausanne, Switzerland, when part of this work was carried out. U.K. was an employee of Merck KGaA, Darmstadt, Germany, when this work was carried out, but currently, U.K. is at CureVac GmbH.

Author Contributions. N.T., P.G., U.K., and A.M. wrote the manuscript. N.T., P.G., U.K., and A.M. designed the research. N.T. and K.I. performed the research. N.T. and K.I. analyzed the data.

1. EFPIA MID3 Workgroup *et al.* Good practices in model-informed drug discovery and development: practice, application, and documentation. *CPT Pharmacometrics Syst. Pharmacol.* **5**, 93–122 (2016).
2. Bender, B.C., Schindler, E. & Friberg, L.E. Population pharmacokinetic-pharmacodynamic modelling in oncology: a tool for predicting clinical response. *Br. J. Clin. Pharmacol.* **79**, 56–71 (2015).
3. Mould, D.R., Walz, A.C., Lave, T., Gibbs, J.P. & Frame, B. Developing exposure/response models for anticancer drug treatment: special considerations. *CPT Pharmacometrics Syst. Pharmacol.* **4**, e00016 (2015).
4. Claret, L. *et al.* Model-based prediction of phase III overall survival in colorectal cancer on the basis of phase II tumor dynamics. *J. Clin. Oncol.* **27**, 4103–4108 (2009).
5. Tham, L.S. *et al.* A pharmacodynamic model for the time course of tumor shrinkage by gemcitabine + carboplatin in non-small cell lung cancer patients. *Clin. Cancer Res.* **14**, 4213–4218 (2008).
6. Wang, Y. *et al.* Elucidation of relationship between tumor size and survival in non-small-cell lung cancer patients can aid early decision making in clinical drug development. *Clin. Pharmacol. Ther.* **86**, 167–174 (2009).
7. Simeoni, M. *et al.* Predictive pharmacokinetic-pharmacodynamic modeling of tumor growth kinetics in xenograft models after administration of anticancer agents. *Cancer Res.* **64**, 1094–1101 (2004).
8. Rocchetti, M. *et al.* Predictive pharmacokinetic-pharmacodynamic modeling of tumor growth after administration of an anti-angiogenic agent, bevacizumab, as single-agent and combination therapy in tumor xenografts. *Cancer Chemother. Pharmacol.* **71**, 1147–1157 (2013).
9. Terranova, N., Germani, M., Del Bene, F. & Magni, P. A predictive pharmacokinetic-pharmacodynamic model of tumor growth kinetics in xenograft mice after administration of anticancer agents given in combination. *Cancer Chemother. Pharmacol.* **72**, 471–482 (2013).
10. Ribba, B. *et al.* A review of mixed-effects models of tumor growth and effects of anticancer drug treatment used in population analysis. *CPT Pharmacometrics Syst. Pharmacol.* **3**, e113 (2014).

11. Bruno, R. & Claret, L. On the use of change in tumor size to predict survival in clinical oncology studies: toward a new paradigm to design and evaluate phase II studies. *Clin. Pharmacol. Ther.* **86**,136–138 (2009).
12. James, K. *et al.* Measuring response in solid tumors: unidimensional versus bidimensional measurement. *J. Natl. Cancer Inst.* **91**, 523–528 (1999).
13. World Health Organization. *WHO Handbook for Reporting Results of Cancer Treatment* (Geneva, Switzerland, World Health Organization, 1979).
14. Park, J.O. *et al.* Measuring response in solid tumors: comparison of RECIST and WHO response criteria. *Jpn. J. Clin. Oncol.* **33**, 533–537 (2003).
15. Eisenhauer, E.A. *et al.* New response evaluation criteria in solid tumours: revised RECIST guideline (version 1.1). *Eur. J. Cancer* **45**, 228–247 (2009).
16. Sharma, M.R., Maitland, M.L. & Ratain, M.J. RECIST: no longer the sharpest tool in the oncology clinical trials toolbox—point. *Cancer Res.* **72**, 5145–5149; discussion 5150 (2012).
17. Terranova, N., Girard, P., Klinkhardt, U. & Munafo, A. Resistance development: a major piece in the jigsaw puzzle of tumor size modeling. *CPT Pharmacometrics Syst. Pharmacol.* **4**, 320–323 (2015).
18. Bedard, P.L., Hansen, A.R., Ratain, M.J. & Siu, L.L. Tumour heterogeneity in the clinic. *Nature* **501**, 355–364 (2013).
19. Kim, M., Gillies, R.J. & Rejniak, K.A. Current advances in mathematical modeling of anti-cancer drug penetration into tumor tissues. *Front. Oncol.* **3**, 278 (2013).
20. Foo, J. & Michor, F. Evolution of acquired resistance to anti-cancer therapy. *J. Theor. Biol.* **355**, 10–20 (2014).
21. Wei, W.W.W. *Time Series Analysis. Univariate and Multivariate Methods. Second Edition* (Reading, MA, Addison-Wesley, 1994).
22. MacQueen, J. Some methods for classification and analysis of multivariate observations. *Proc. Fifth Berkeley Symp. Math. Statist. Prob.* **1**, 281–297 (1967).
23. Wilke, H. *et al.* Cetuximab plus irinotecan in heavily pretreated metastatic colorectal cancer progressing on irinotecan: MABEL study. *J. Clin. Oncol.* **26**, 5335–5343 (2008).
24. Van Cutsem, E. *et al.* Inpatient cetuximab dose escalation in metastatic colorectal cancer according to the grade of early skin reactions: the randomized EVEREST study. *J. Clin. Oncol.* **30**, 2861–2868 (2012).
25. Burrell, R.A., McGranahan, N., Bartek, J. & Swanton, C. The causes and consequences of genetic heterogeneity in cancer evolution. *Nature* **501**, 338–345 (2013).
26. Ogino, S., Fuchs, C.S. & Giovannucci, E. How many molecular subtypes? Implications of the unique tumor principle in personalized medicine. *Expert Rev. Mol. Diagn.* **12**, 621–628 (2012).
27. Fritz, A. *et al.* eds. *International Classification of Diseases for Oncology. Third Edition* (Geneva, Switzerland, World Health Organization, 2000).

© 2018 The Authors CPT: Pharmacometrics & Systems Pharmacology published by Wiley Periodicals, Inc. on behalf of American Society for Clinical Pharmacology and Therapeutics. This is an open access article under the terms of the Creative Commons Attribution-NonCommercial License, which permits use, distribution and reproduction in any medium, provided the original work is properly cited and is not used for commercial purposes.

Supplementary information accompanies this paper on the *CPT: Pharmacometrics & Systems Pharmacology* website (<http://psp-journal.com>)